Journal of Turbomachinery. Received June 29, 2020;
Accepted manuscript posted January 19, 2021. doi:10.1115/1.4050114

EFFECT OF RADIATION ON HEAT TRANSFER INSIDE AEROENGINE COMPRESSOR ROTORS

Hui Tang* and J Michael Owen

Department of Mechanical Engineering, University of Bath, BA2 7AY, Unite Kingdom

E-mail@ h.tang2@bath.ac.uk

Abstract

The blade clearance in aero-engine compressors is mainly controlled by the radial growth of the compressor discs, to which the blades are attached. This growth depends on the radial distribution of the disc temperature, which in turn is determined by the heat transfer inside the internal rotating cavity between adjacent discs. The buoyancy-induced convection inside the cavity is significantly weaker than that associated with the forced convection in the external mainstream flow, and consequently radiation between the cavity surfaces cannot be ignored in the calculation of the disc temperatures. In this paper, both the Monte Carlo Ray-Trace Method and the view factor method are used to calculate the radiative flux when the temperatures of the discs, shroud and inner shaft of the compressor vary radially and axially. The Monte Carlo Ray-Trace method is computationally expensive, but it is able to incorporate the effect of complex geometries on radiation. The view factor method is quick to compute and, although the derivation becomes complicated when geometrical details are considered, it can be used as a first check of the effect of radiation in compressor cavities. Given distributions of surface temperatures, the blackbody and grey body heat fluxes were calculated for the discs, shroud and inner shaft in two experimental compressor rigs and in a simulated compressor stage. For the experimental rigs, although the effect of radiation was relatively small for the case of large Grashof numbers, the relative effect of radiation increases as Gr (and consequently the convective heat transfer) decreases. For the simulated compressor, with a pressure ratio of 50:1 for state-of-art aircraft engines, radiation could have a significant effect on the disc temperature and consequently on the blade clearance; the effect is predicted to be more prominent for next generation of aircraft engines with pressure ratios up to 70:1.

1. Introduction

Fig. 1 shows a simplified diagram of a high-pressure aero-engine compressor. A compressor rotating cavity is formed by two adjacent discs and a shroud, and cooling air extracted from the compressor mainstream flows axially between the disc cobs and the inner shaft. In aero-engines, often there is an axial gap between the cobs of

the two adjacent discs, in which case, the cavity is referred to as the "open" cavity. In some industrial gas turbines, it is possible that the gap is closed off, and the cavity is referred to as the "closed" cavity.

As compressor pressure ratios increase above 50:1, the height of the blades decreases and the size of the clearance between the blades and the outer casing becomes increasingly important. The clearance is mainly controlled by the radial growth of the compressor discs to which the blades are attached, and the growth depends not only on the temperature *level* but also on the *radial distribution* of the disc temperature, which is in turn determined by the heat transfer in the compressor cavity.

Under steady-state operating conditions, the shroud and the discs are hotter than the axial through flow of cooling air. Under these conditions, buoyancy-induced flow occurs inside the rotating cavity, and the convective heat transfer tends to be significantly less than that associated with the forced convection in other parts of the engine. Consequently, the effect of radiant heat transfer between the rotating surfaces surrounding the cavity cannot be ignored.

A detailed review of buoyancy-induced flow in open and closed rotating cavities is given by Owen and Long [1]. Buoyancy-induced flow is a conjugate problem in which the flow is controlled by the temperature distribution on the discs and the temperature is controlled by the flow in the cavity. Experiments have been conducted to investigate the buoyancy-induced heat transfer in compressor cavities. Bohn *et al.* [2] measured the heat transfer in "closed" compressor cavities, and Bohn *et al.* [3] investigated the heat transfer from "open" compressor discs. Atkins and Kanjirakkad [4] measured the disc temperatures at different experimental conditions in a multi-cavity compressor rig at the University of Sussex. Using these temperatures, Tang *et al.* [5] calculated the radial distribution of the disc heat transfer by applying Bayesian statistics in conjunction with the solution of the circular fin equation for conduction in the compressor disc. Jackson et al. [6] measured the disc temperatures on a compressor rig at the University of Bath, and they calculated the disc heat transfer using the Bayesian method as Tang *et al.* [5]. The temperature profiles were reproduced using the theoretical buoyancy model developed by Owen and Tang [7]. Luberti et al. [8] used the theoretical model to predict the temperature profiles and heat transfer of compressor cavities for state-of-art engines at pressure ratios at 50:1 and next generation of engines at pressure ratios up to 70:1. Though many studies have been published on the buoyancy-induced heat transfer inside compressor cavities, there are few detailed investigations of the effect of the radiation, which was either neglected [2,3,9] or only briefly stated [10,11]. This paper evaluates the effect of radiation on the heat transfer in the experimental compressor cavities used by Bohn et al. [2] and Jackson et al. [6] and the simulated aero-engine cavity used by Luberti et al. [8].

Incropera & De Witt [12] and Modest [13] provided a comprehensive background for radiative heat transfer. Given the surface temperatures and the view factors, the radiation exchange between surfaces in compressor cavities can be calculated. Analytical equations can be found for the *elemental view factors*, $f_{i,j}$, for disc annuli and cylindrical rings, considering the blockage by an inner cylinder [14]. This view factor (VF) method is fast to calculate but limited to simple cavity geometries. Mathematical derivation becomes complex when geometrical details, such as fillets and cobs, are considered.

The Monte Carlo Ray-Trace (MCRT) method is widely used to calculate radiation for complex geometries, and a detailed review of the method is given in [15] and [13]. It is a statistical method and, though being computationally expensive, MCRT is able to accurately incorporate comprehensive effects in estimating radiative heat transfer, including participating media, spectral dependence and complex geometries [15]. Besides, advances have been made to reduce the computational time [16,17]. In this paper, MCRT in a CFD (Computational Fluid Dynamics) software package is used to estimate the radiative heat flux in compressor cavities, considering the blockage effect of the cob geometries, and it is compared with the VF method using simplified cavity geometries.

Section 2 presents the methodology of using the VF and MCRT methods to calculate the radiation in compressor cavities. Section 3 discusses the convection in compressor cavities, and Section 4 compares the radiation and convection in a closed and open cavity experimental compressor rigs as well as a simulated aero-engine compressor cavity. The main conclusions are summarised in Section 5, and the appendix includes the detailed calculations of view factors applicable to axisymmetric conditions.

2. Calculation of radiation in compressor cavities

2.1 View factor (VF) method for radiation in closed compressor cavities

For compressor cavities, the circumferential variation of the temperature is negligible compared with the variation in the axial and radial directions. The disc, shroud and shaft can be divided into a number of isothermal annuli or ring elements. The elemental view factors for elements i and j, $f_{i,j}$, can be calculated using

$$f_{i,j} = \frac{1}{dA_i}\int_{dA_i}\int_{dA_j}\frac{\cos\theta_i \cos\theta_j}{\pi R^2} d\alpha_i d\alpha_j \quad (1)$$

where dA_i and dA_j are the area of the ring elements, $d\alpha_i$ and $d\alpha_j$ are the sub-elements, R is the distance between sub-elements $d\alpha_i$ and $d\alpha_j$, and θ_i and θ_j denote the angles between the line connecting $d\alpha_i$ and $d\alpha_j$ and the normals to $d\alpha_i$ and $d\alpha_j$.

For closed cavity geometries in Fig. 2, the elemental view factors can either be derived from the listed analytical view factors in [14] or directly calculated using eq. 1. The appendix presents the detailed calculations of the elemental view factors using the second method.

For radiation exchange between a limited number of opaque, diffuse, grey, isothermal surface elements of a closed cavity, the irradiation at element i, G_i, is the sum of emitted and reflected radiation from all elements of the cavity [12]. It follows

$$G_i = \sum_{j=1}^{N} f_{i,j}\left[\varepsilon_j \sigma T_j^4 + (1-\varepsilon_j) G_j\right] \tag{2}$$

where N is the total number of ring elements, and eq. (2) can be solved using matrix inversion. The grey body radiative flux at element dA_i is

$$q_i = \varepsilon_i \sigma T_i^4 - \varepsilon_i G_i \tag{3}$$

A special case of eq. (3) is the blackbody radiative flux, which is calculated using

$$q_i = \sum_{j=1}^{N} f_{i,j} \sigma (T_i^4 - T_j^4) \tag{4}$$

Once the view factors are determined and the temperature variation is given, the grey body radiative heat flux can be calculated in microseconds using a laptop.

For the compressor cavities in aircraft engines, the cob and fillets lead to more complex cavity geometry, and often during the design process the geometry can be changed. In experimental studies of heat transfer in compressor cavities, it is required to estimate the effect of radiation at different experimental conditions. In section 4, it is shown that the geometry can be simplified into a closed cavity and the calculated radiative heat flux can be used as a preliminary check of the effect of radiation on heat transfer inside compressor cavities.

2.2 Monte Carlo Ray Trace (MCRT) method

The Monte Carlo model in the ANSYS CFX software is used to simulate the radiation exchange between grey surfaces of compressor cavities. The model uses the MCRT algorithm to track the photon histories [18]. The full three-dimensional geometry of the cavity is used, and the radiative heat flux is averaged circumferentially. This can reduce the number of histories (or rays) required for accurate estimation.

2.2.1 Test cases

The radiation in a closed cavity in [2], an experimental open cavity in [6], and an engine open cavity in [8] are modelled using MCRT in this study. The cavity geometries are illustrated in Fig. 2, and key geometrical parameters are provided in Table 1. Surface temperatures are specified at different axial and radial locations, and the ranges of shroud and inner cylinder surface temperatures are given in Table 1. For the closed cavity in [1], the disc temperature is assumed to be the average of the shroud and the inner cylinder temperatures. For open cavities in [6] and [8], radial distributions of the disc temperatures are used, the shaft temperature is assumed to be the same with the through flow air temperature, and the inlet and outlet of the cavity are treated as open boundaries where no emission or refection occurs. The mesh size, 0.0042 m, and the number of histories, 10^7, are selected to ensure the accuracy of the calculation. The flow is not simulated in these calculations. The radiative heat transfer in a closed cavity with $T_{sh} = 341\ K$ and $T_c = 288\ K$ is used here to illustrate the effect of the mesh size and the number of histories on the calculated radiative heat fluxes.

2.2.2 Effect of surface mesh size

Note that as the medium inside these cavities is transparent, the calculation of the radiative fluxes is determined by surface meshes only. (It should be noted that if a participating medium is considered, radiation tends to be attenuated [19,20].) Table 2 shows the effect of the surface mesh size on the average radiative heat fluxes on the inner cylindrical surface. The radiative heat flux calculated using 10^7 histories and different mesh sizes are compared with the analytical value, which is calculated using the analytical view factors listed in [14]. Also listed is the result calculated using the elemental view factors derived in the appendix. The agreement between the analytical and calculated fluxes supports the validation of the VF and the MCRT methods for radiation in closed cavities. The mesh size 0.0042 m was selected to reach an accuracy of 0.2% in estimating heat fluxes.

2.2.3 Effect of number of histories

The accuracy of the spatial distribution of the radiative heat flux using MCRT is highly dependent on the number of photon histories. Figure 3 shows that at the mesh size of 0.0042 m and using 10^7 histories, the radial distribution of the radiative heat flux on compressor discs is smooth and agrees well with the results calculated using the view factor method.

3. Convection in compressor cavities

Journal of Turbomachinery. Received June 29, 2020;
Accepted manuscript posted January 19, 2021. doi:10.1115/1.4050114

As discussed above, under steady-state engine-operating conditions, the heat transfer inside compressor cavities is dominated by the buoyancy-induced convection. The convection depends mainly on the Grashof number, Gr, where

$$Gr = Re_{\phi}^{2}\Delta T/T_{ref} \tag{5}$$

where Re_{ϕ} is the rotational Reynolds number and ΔT is the temperature difference between the shroud and the reference temperature T_{ref}. It is shown in [1] that Nu tends to increase as Gr increases. However, under some transient engine-operating conditions the temperature of the shroud can be lower than that of the axial throughflow. This can lead to *thermally-stratified flow* where convection could be significantly reduced and, in theory, could be less than the radiant heat transfer (see Owen & Long [1]).

Owen and Tang [7] developed a theoretical model for buoyancy-induced flow and heat transfer in compressor cavities; the model was based on Ekman-layer flow on the discs and compressible flow in the fluid core between the discs. The model, which was validated by Tang and Owen [21], showed that the root mean square (RMS) error between the calculated and measured average Nusselt numbers was less than 10%, and between the disc temperatures it was less than 3%. The authors also showed that, for a constant value of Gr, the buoyancy-induced heat transfer can be significantly reduced as Re_{ϕ} increases, owing to the compressible flow in the core. The compressibility effect was graphically shown in the experimental data of Jackson et al. [6], where the Owen-Tang buoyancy model was used to predict the disc temperatures in the compressor rig.

The buoyancy model was also used to predict the temperatures used by Luberti et al. [8] to calculate the radial growth of the discs in a simulated compressor stage with overall pressure ratios of 50:1, 60:1 and 70:1. These authors showed that the effect of the radial distribution of temperatures on the disc growth was of the same magnitude as the blade clearance itself. Consequently, when radiation is of the same magnitude as the convection then radiation can have a significant effect on the disc temperature distribution and therefore on the blade clearance.

The geometries of the cavities used in [2], [6] and [8] are shown in Figure 2 and key geometrical parameters are given in Table 1. The closed cavity geometry is also used as the simplified version of the two open cavities for the view factor method to estimate the radiative heat fluxes. For the simplified cavities, the temperatures of the inner cylinder and disc surfaces at $r < r_a$ are assumed to be the same with the temperature of the axial throughflow.

4. Effect of radiation on heat transfer in compressor cavities

The radiative heat flux in the closed and open cavities can be estimated using the methodology given in Section 2.

4.1 Experimental closed cavity rig

In [2], the total (convective and radiative) heat transfer from the heated outer cylindrical surface to the cooled inner cylindrical surface of three different closed cavities was measured for a range of rotational speeds and temperature differences between the two surfaces. The maximum rotational speed and temperature difference was 3500 rpm and 85 C respectively, and both disc surfaces were insulated. For the results presented here, blackbody and grey body radiation were calculated using both the VF and MCRT methods in cavity B, the geometrical parameters of which are given in Table 1. For the grey body radiation, the emissivity is assumed to be that of dull copper surfaces, 0.25 [22], which is to simulate the condition of the copper shroud after long exposures in air.

A "total" Nusselt number for the total heat flux on the inner cylinder ($q_{tot,c}$) is defined as

$$Nu \stackrel{\text{def}}{=} \frac{q_{tot,c} r_c \, ln\frac{r_{sh}}{r_c}}{k\Delta T} \tag{6}$$

where ΔT is the temperature difference between the shroud and the inner cylinder. An equivalent Nusselt number for the radiative heat transfer on the inner cylindrical surface ($q_{rad,c}$) is defined as

$$Nu_{rad} \stackrel{\text{def}}{=} \frac{q_{rad,c} r_c \, ln\frac{r_{sh}}{r_c}}{k\Delta T} \tag{7}$$

It should be noted that

$$q_{tot,c} = q_{rad,c} + q_{conv,c} \tag{8}$$

Instead of the Grashof number, the Rayleigh number, Ra, was used, which is defined as

$$Ra \stackrel{\text{def}}{=} PrRe_{\phi}^2 \frac{\Delta T}{T_{ref}} \frac{(r_{sh} - r_c)^3 (r_{sh} + r_c)}{2r_{sh}^4} \tag{9}$$

where the reference temperature is the average of the temperatures of the shroud and the inner cylinder. The relationship between Ra and Gr is

$$Ra = PrGr \frac{(r_{sh} - r_c)^3 (r_{sh} + r_c)}{2r_{sh}^4} \tag{10}$$

Fig. 4 compares the estimated equivalent Nusselt number for blackbody radiation and grey body radiation with $\varepsilon = 0.25$ to the measured total Nusselt number. It can be seen that at low Ra, the calculated blackbody radiative heat fluxes can be higher than that of convection, and the grey body fluxes can account for more than 30% of the total heat fluxes. This shows that radiation in experimental rigs cannot be ignored at low Ra conditions.

4.2 Experimental compressor cavity rig

In [6], the radial distribution of the temperatures of the upstream and downstream discs was measured at different experimental conditions, and the total (convective and radiative) heat fluxes were determined using the Bayesian method developed in [5]. As the upstream and downstream discs were symmetrically heated, there was little difference between the two temperature distributions. All surfaces in the cavity and on the shaft were painted matt black, hence blackbody radiation was assumed. (Black surfaces increase the effect of radiation; however, owing to the uncertainty in the value of the emissivity of most metals, black surfaces provide greater certainty in the radiation calculations.)

Both the VF method with simplified cavity geometry and the MCRT method with the actual cavity were used to calculate the radiation on the discs, shroud and inner shaft. Fig. 5 compares the calculated disc radiative fluxes with the convective heat flux determined from the measured disc temperature distribution given in [6]. This was an experimental case where the Grashof number was large ($Gr = 2 \times 10^{12}$), and consequently the convective flux was much larger than the radiative flux. (Although it is not reported here, the effect of radiation was significant in experiments conducted at low rotational speeds and low Grashof numbers.)

There is good agreement between the radiative fluxes calculated by the VF and MCRT methods except near the cob region. The difference in the total radiative heat flow is less than 10%, which results in a 0.5% difference in the averaged dimensionless disc temperature. It shows that the view factor method with simplified cavity geometry can be used as a preliminary check for the effect of radiation on the heat transfer inside compressor cavities.

4.3 Convection and radiation for a simulated compressor cavity

These calculations were based on the geometry given in Table 1 and on the temperatures used by Luberti et al. [8] for a disc in a simulated high-pressure compressor with state-of-art and next generation aero-engine overall pressure ratios (OPR) of 50:1 and 70:1 respectively. The simulations in [8], which were based on the cruise conditions with a flight Mach number of 0.85 and an altitude of 10,000 m, used the Owen-Tang buoyancy model in [7] to calculate the convective fluxes and disc temperature, but radiation was not considered. In the radiation

calculations made here, it was assumed that both discs in the cavity had the same temperature distribution, and blackbody and grey body radiation with $\varepsilon = 0.75$ are calculated. The emissivity of 0.75 was selected to simulate the emissivity of the oxidised Inconel 718 at about 800K as given in [23] and [24].

Fig. 6 compares radiation with convection for a high-pressure compressor cavity at 50:1 pressure ratio ($Gr = 1.2 \times 10^{13}$), and it can be seen that the relative effect of radiation is significant. Although grey-body radiative fluxes would be lower than the blackbody ones calculated here, radiation could still have a significant effect due to the oxidisation. As shown in Fig. 7, for a pressure ratio of 70:1 for the next generation of aero-engines ($Gr = 1.7 \times 10^{13}$), radiation shows a more prominent effect. Note that the discontinuous behaviour of the radiative heat flux is caused by the sudden decrease of disc thickness near the cob region, which is shown by the disc silhouette in Fig. 6.

At different engine-operating conditions, the convection in compressor cavities could be further reduced not only at lower rotational speed but also, owing to compressibility effects, at higher rotational speed. In addition, owing to the increase of the air temperature, the relative effect of radiation could be increased at lower altitudes.

5 Conclusions

The effect of radiation on heat transfer inside an experimental closed cavity rig, an experimental open cavity rig and a simulated aeroengine cavity has been investigated. The view factor method and the Monte Carlo Ray-Trace method were used to calculate the blackbody and grey body radiative heat fluxes on the shroud, disc and inner cylindrical surfaces. The comparison between estimated radiation and measured heat transfer in experimental closed cavities demonstrated that, at small Gr numbers, where convection is relatively low, radiation can account for more than 30% of the total heat transfer. For experimental open cavities, the good agreement between the radiative heat fluxes calculated using the VF method and the MCRT method illustrated that the VF method with simplified cavity geometries can be used as an efficient way of estimating the effect of radiation. For the simulated compressor, with a pressure ratio of 50:1, the effect of radiation could be significant in the calculation of the radial distribution of disc temperature (and consequently on the blade clearance); as the pressure ratio increases, the cavity surface temperature increases and the relative effect of radiation becomes increasingly important. In addition, owing to the increase of the air temperature, the relative effect of radiation could become more significant at lower altitudes (e.g. under take-off conditions). Moreover, as discussed in Section 3, Owing to compressibility effects in the compressor cavity, convection will decrease as the rotational speed increases,

Journal of Turbomachinery. Received June 29, 2020;
Accepted manuscript posted January 19, 2021. doi:10.1115/1.4050114

which in turn increases the relative effect of radiation. Consequently, the effect of radiation should be carefully assessed when calculating the heat transfer in experimental cavity rigs and aero-engine compressor cavities.

Appendix: Calculation of elemental view factors

Fig. 8 shows the geometries used for the calculations of the elemental view factors for five different cases: from disc to disc; from disc to shroud; from shroud to shroud; from disc to inner cylinder; and from shroud to inner cylinder. The shading effect caused by the presentence of the inner cylinder is also considered. As discussed in Section 2.1, the elemental view factors between dA_i and dA_j, $f_{i,j}$ can be calculated using the direct integration in eq.1. Considering the axisymmetric geometries in this study, eq. 1 is equivalent to

$$f_{i,j} = r_j dl_j \int_0^{\Phi_{i,j}} \frac{\cos\theta_i \cos\theta_j}{\pi R^2} d\phi_j \tag{A1}$$

where l is the span of the elements on the r-z plane and $\Phi_{i,j}$ is the angle where the blockage of the inner cylinder occurs. The detailed calculations of the view factors for all cases are listed in Table 3. Eqs. A2-A9 used in the table are given below.

$$R = \sqrt{{r_i}^2 + {r_j}^2 - 2r_i r_j \cos\phi_j + (z_i - z_j)^2} \tag{A2}$$

$$\cos\theta = s/R \tag{A3}$$

$$\cos\theta = \frac{z_j - z_i}{R} \tag{A4}$$

$$\cos\theta = \frac{r_i - r_j \cos\phi_j}{R} \tag{A5}$$

$$\cos\theta = \frac{r_j - r_i \cos\phi_j}{R} \tag{A6}$$

$$\cos\theta = \frac{r_i \cos\phi_j - r_j}{R} \tag{A7}$$

$$\Phi_{i,j} = \arccos\frac{r_c}{r_i} + \arccos\frac{r_c}{r_j} \tag{A8}$$

$$\Phi_{i,j} = \arccos\frac{r_c}{r_i} \tag{A9}$$

The calculated elemental view factors are validated using the analytical values listed in [14]. The analytical view factors are also used to calculated analytical radiative heat fluxes in closed cavities (see Table 2 and Fig. 4).

Journal of Turbomachinery. Received June 29, 2020;
Accepted manuscript posted January 19, 2021. doi:10.1115/1.4050114

Nomenclature

A	area
f	elemental view factors
Gr	Grashof number ($= Re_\phi^2 \Delta T / T_{ref}$)
l	span of the elements on the r-z plane
k	thermal conductivity of air
Nu	Nusselt number
q	heat flux
r	radius
R	distance between $d\alpha_i$ to $d\alpha_j$
Ra	Rayleigh number
Re_ϕ	rotational Reynolds number ($= \rho \Omega r_{sh}^2 / \mu$)
s	axial space between discs
T	temperature
z	axial location
ΔT	temperature difference
θ	angle between the normal to $d\alpha$ and R
μ	dynamic viscosity
ρ	density
σ	Stefan-Boltzmann constant
ϕ	circumferential coordinates
Φ	shading parameter
Ω	rotational speed

Subscripts

c	inner cylinder
$conv$	convective heat transfer
i	radiating surface
j	irradiated surface
rad	radiative heat transfer

ref	reference
sh	shroud
tot	total values

References

[1] Owen, J. M. and Long, C. A., 2015, "Review of Buoyancy-Induced Flow in Rotating Cavities," ASME J. Turbomach., 137(11), 111001.

[2] Bohn, D., Deuker, E., Emunds, R. and Gorzelitz, V., 1995, Experimental and Theoretical Investigations of Heat Transfer in Closed Gas-Filled Rotating Annuli," ASME J. Turbomach., 117(1), 175-183.

[3] Bohn, D. E., Deutsch, G. N., Simon, B. and Burkhardt C., 2000, "Flow Visualisation in a Rotating Cavity with Axial Throughflow," ASME Paper 2000-GT-0280.

[4] Atkins, N. R., and Kanjirakkad, V., 2014, "Flow in a Rotating Cavity with Axial Throughflow at Engine Representative Conditions," ASME Paper GT2014-27174.

[5] Tang, H. and Owen, J.M., 2016, "Effect of Buoyancy-Induced Flow on Temperatures of Compressor Discs," ASME J. Eng. Gas Turbines Power, 139(6), 1-10.

[6] Jackson, R. W., Luberti, D., Tang, H., Pountney, O. J., Scobie, J. A., Sangan, C. M., Owen, J. M., and Lock, G. D., 2020, "Measurement and analysis of buoyancy-induced heat transfer in aero-engine compressor rotors," ASME paper GT2020-14427.

[7] Owen, J. M., and Tang, H., 2015, "Theoretical Model of Buoyancy-Induced Flow in Rotating Cavities," ASME. J. Turbomach., 137(11), p. 111005.

[8] Luberti, D., Tang, H., Scobie, J.A., Pountney, O.J., Owen, J.M. and Lock, G.D., 2020, "Influence of Temperature Distribution on Radial Growth of Compressor Disks," Journal of Engineering for Gas Turbines and Power, 142(7).

[9] Günther, A, Uffrecht, W and Odenbach, S, 2014, "The Effects of Rotation and Mass Flow on Local Heat Transfer in Rotating Cavities with Axial Throughflow," ASME Paper GT2014-26228.

[10] Long, C. A., Morse, A. P., and Tucker, P. G., 1997, "Measurement and Computation of Heat Transfer in High-Pressure Compressor Drum Geometries With Axial Throughflow," ASME. J. Turbomach, 119(1): 51–60.

[11] Long, C. A., and Childs, P. R. N., 2007, "Shroud Heat Transfer Measurements Inside a Heated Multiple Rotating Cavity with Axial Throughflow," Int. J. Heat Fluid Flow, 28(6), pp. 1405–1417.

[12] Incropera, F. P., and DeWitt, D. P., 1996, "Introduction to Heat Transfer," JohnWiley, New York.

[13] Modest, M. F., 2013. "Radiative Heat Transfer," Elsevier.

[14] Howell, J. R., and Mengüç, M. P., 2011, "Radiative Transfer Configuration Factor Catalog: A Listing of Relations for Common Geometries," J. Quantitative Spectroscopy and Radiative Transfer, 112(5), 910-912.

[15] Howell, J. R., 1998, "the Monte Carlo Method in Radiative Heat Transfer," ASME J. Heat Trans., 120(8), 547-560.

[16] Morokoff, W. J. and Caflisch, R. E. 1995, "Quasi-Monte Carlo Integration," J. Computational Phys., vol. 122, pp. 218–230.

[17] Palluotto, L., Dumont, N., Rodrigues, P., Gicquel, O., and Vicquelin, R., 2019, "Assessment of Randomized Quasi-Monte Carlo Method Efficiency in Radiative Heat Transfer Simulations," Journal of Quantitative Spectroscopy and Radiative Transfer, 236:106570.

[18] ANSYS, 2019, "ANSYS CFX Solver Manual", CFX-19.

[19] Colomer, G., Costa, M., Consul, R. and Oliva. A., 2004, "Three-Dimensional Numerical Simulation of Convection and Radiation in a Differentially Heated Cavity Using the Discrete Ordinates Method," Int. J. Heat Mass Transf., 47(2), 257-269.

[20] Soucasse, L., Rivière, Ph., Soufiani, A., Xin, S. and Le Quéré, P., 2014, "Transitional Regimes of Natural Convection in a Differentially Heated Cubical Cavity under the Effects of Wall and Molecular Gas Radiation," Physiscs of Fluids, 26, 024105.

[21] Tang, H. and Owen, J.M., 2017, "Effect of Buoyancy-Induced Flow on Temperatures of Compressor Discs," ASME J. Eng. Gas Turbines Power, 139(6), 062506.

[22] CIBSE, 2015, "Environmental Design - CIBSE Guide A (8th Edition)", CIBSE.

[23] Greene, G. A., Finfrock, C. C., and Irvine Jr, T. F., 2000, "Total Hemispherical Emissivity of Oxidized Inconel 718 in the Temperature Range 300–1000 C," Eep. Therm. Fluid Sci., 22(3-4), 145-153.

[24] Keller, B. P., Nelson, S. E., Walton, K. L., Ghosh, T. K., Tompson, R. V., and Loyalka, S. K., 2015, "Total Hemispherical Emissivity of Inconel 718," Nucl. Eng. Des. 287, 11-18.

Journal of Turbomachinery. Received June 29, 2020;
Accepted manuscript posted January 19, 2021. doi:10.1115/1.4050114

		r_{sh} (m)	r_c (m)	r_a (m)	s (m)	T_{sh} (K)	T_c (K)
Closed cavity in [2]		0.125	0.24	Not applicable	0.12	312~341	288
Open cavity in [6]		0.052	0.240	0.070	0.040	308	373
Open cavity in [8]	OPR = 50:1	0.074	0.100	0.314	0.061	800	553
	OPR = 70:1					882	612

Table 1: Dimensions and temperatures used in calculations

Journal of Turbomachinery. Received June 29, 2020;
Accepted manuscript posted January 19, 2021. doi:10.1115/1.4050114

Method	Mesh size (m)	Radiation into inner cylinder $q_{rad,c}$ (W/m^2)
Monte Carlo Method (10^7 histories)	0.012	260
	0.0069	266
	0.0042	272
	0.0024	272
	0.0012	272
View factor method	0.0042	272
Analytical results		272

Table 2: Effect of mesh size on the calculated radiative heat flux

Journal of Turbomachinery. Received June 29, 2020;
Accepted manuscript posted January 19, 2021. doi:10.1115/1.4050114

Case	a	b	c	d	e
Geometry	From disc annulus to disc annulus	From disc annulus to shroud ring	From shroud ring to shroud ring	From disc annulus to inner cylinder ring	From shroud ring to inner cylinder ring
$f_{i,j}$	Eq. (A1)				
R	Eq. (A2)				
$\cos\theta_i$	Eq. (A3)	Eq. (A4)	Eq. (A5)	Eq. (A4)	Eq. (A5)
$\cos\theta_j$	Eq. (A3)	Eq. (A6)	Eq. (A5)	Eq. (A7)	Eq. (A7)
l	r	z			
$\Phi_{i,j}$	Eq. (A8)			Eq. (A9)	

Table 3. Elemental view factors for all five cases

Journal of Turbomachinery. Received June 29, 2020;
Accepted manuscript posted January 19, 2021. doi:10.1115/1.4050114

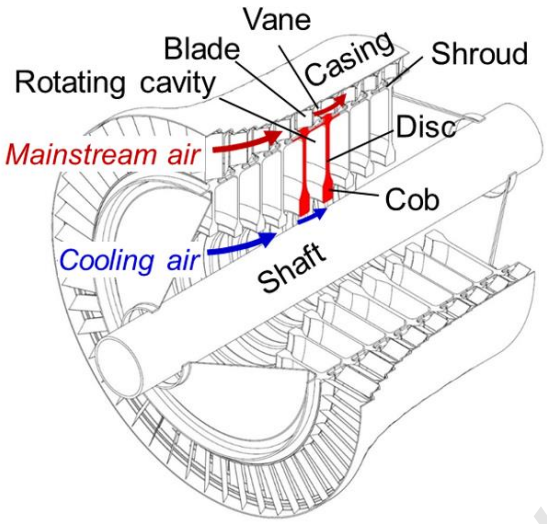

Fig. 1 High-pressure aero-engine compressor

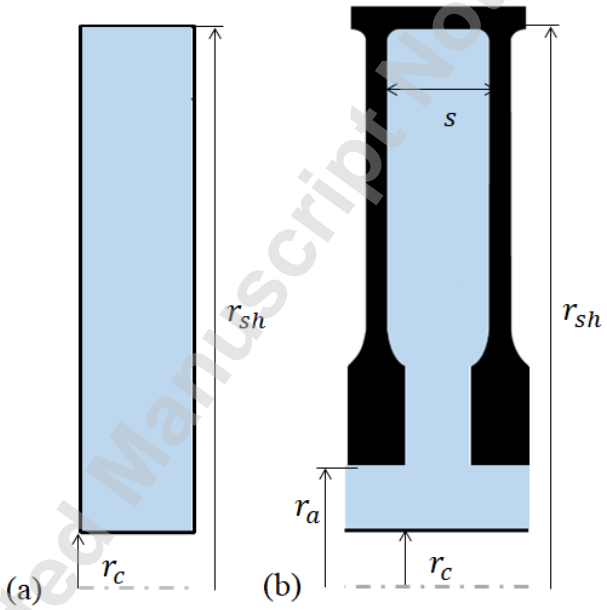

Fig. 2 Geometry used for calculation of radiative and convective heat fluxes: (a) Closed cavity ; (b) Open cavity

Journal of Turbomachinery. Received June 29, 2020;
Accepted manuscript posted January 19, 2021. doi:10.1115/1.4050114

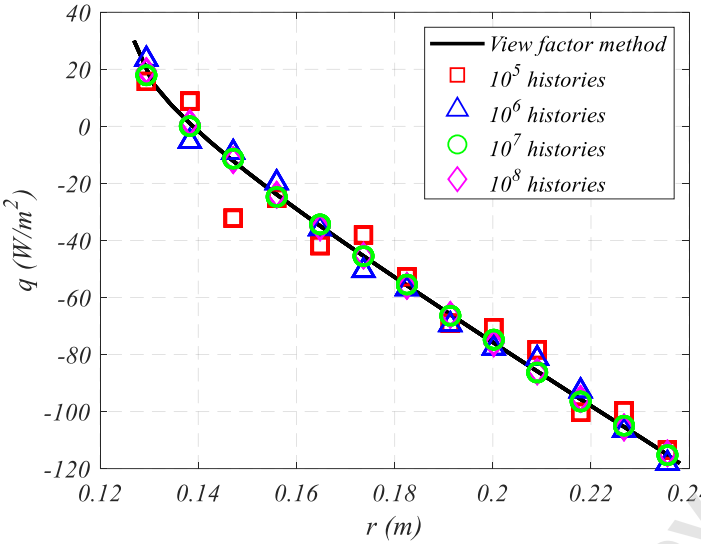

Fig. 3 Effect of the number of histories on the radial distribution of disc radiative heat fluxes (mesh size = 0.0042m).

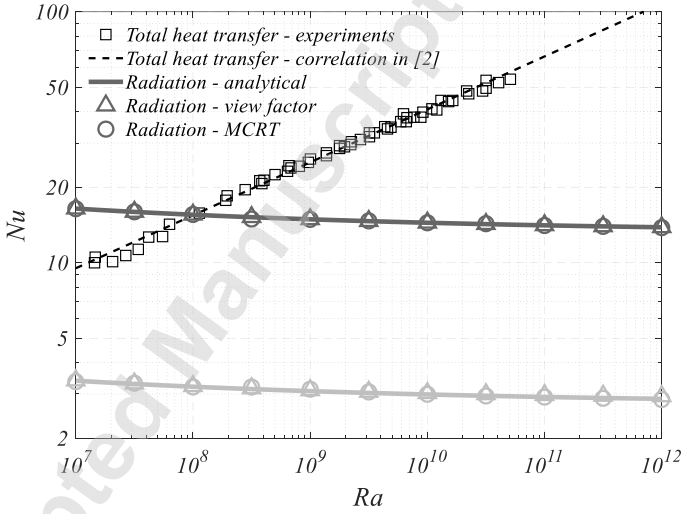

Fig. 4 Comparison between radiative and total heat transfer in a closed cavity. Dark grey: blackbody radiation; Light grey: grey body radiation with $\varepsilon = 0.25$.

Journal of Turbomachinery. Received June 29, 2020;
Accepted manuscript posted January 19, 2021. doi:10.1115/1.4050114

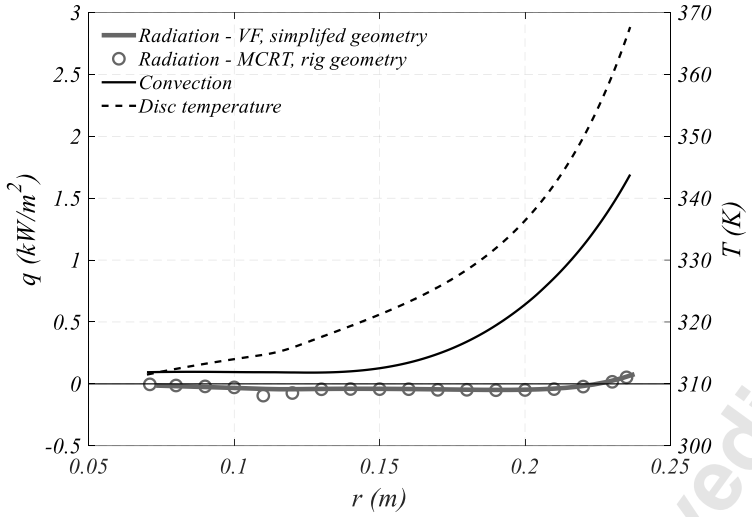

Fig. 5 Calculated radiative and convective heat fluxes for the disc in an experimental rig

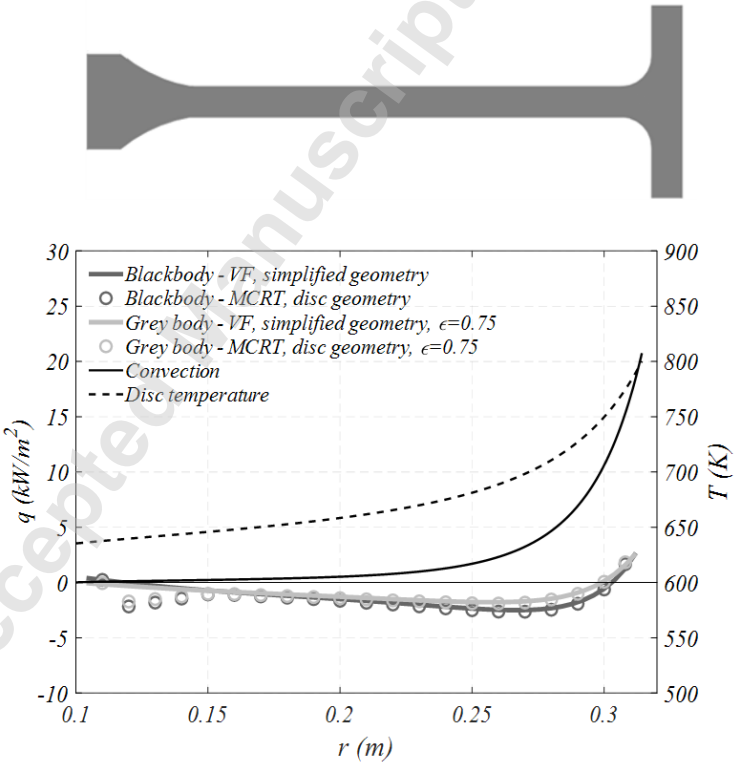

Fig. 6 Calculated radiative and convective heat fluxes for the disc (disc geometry on the top) in a simulated aero-engine compressor cavity with pressure ratio 50:1 ($Gr = 1.2 \times 10^{13}$)

Journal of Turbomachinery. Received June 29, 2020;
Accepted manuscript posted January 19, 2021. doi:10.1115/1.4050114

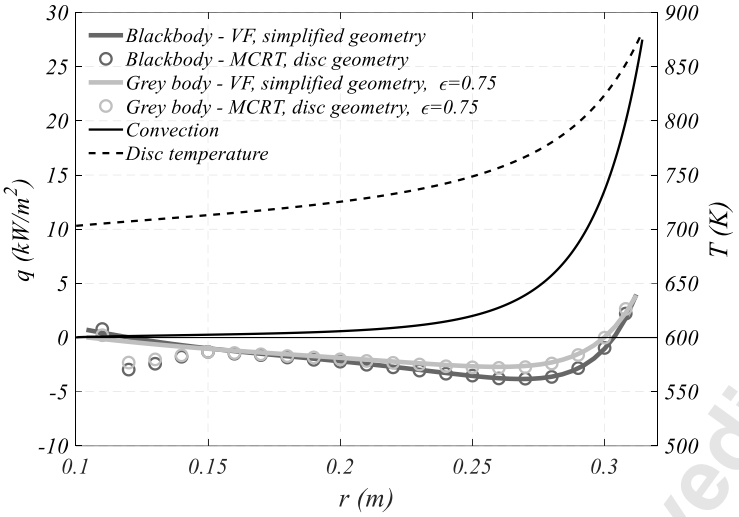

Fig. 7 Calculated radiative and convective heat fluxes for the disc in a simulated aero-engine compressor cavity with pressure ratio 70:1 ($Gr = 1.7 \times 10^{13}$)

Journal of Turbomachinery. Received June 29, 2020;
Accepted manuscript posted January 19, 2021. doi:10.1115/1.4050114

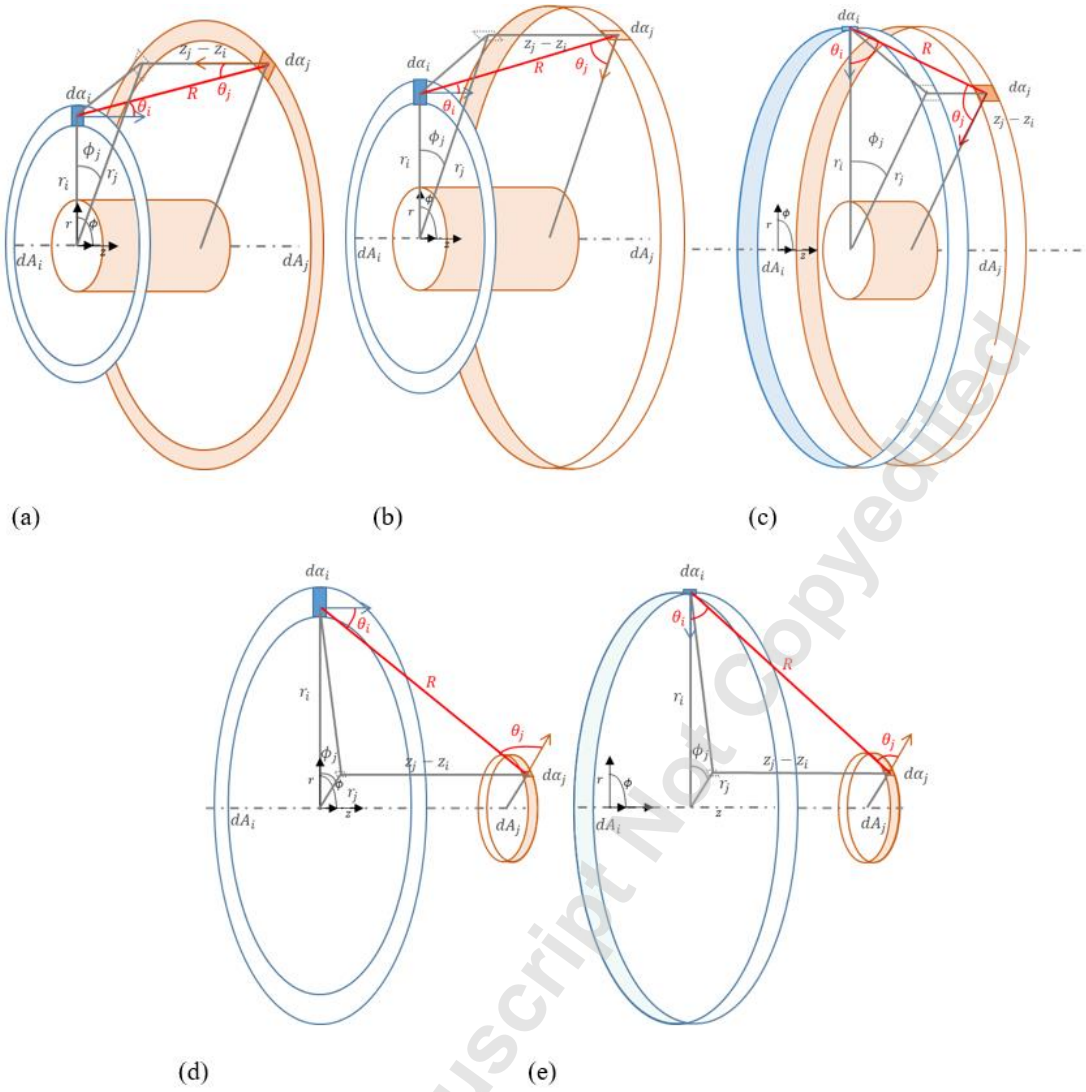

Fig. 8: View factors for (a) disc to disc; (b) disc to shroud; (c) shroud to shroud; (d) disc to inner cylinder; (e) shroud to inner cylinder